



Original article

Novel soluble myeloid cell leukemia sequence 1 (Mcl-1) inhibitor (*E,E*)-2-(benzylaminocarbonyl)-3-styrylacrylonitrile (**4g**) developed using a fragment-based approach

Zhichao Zhang^{a,*}, Ting Song^{b,c,1}, Xiangqian Li^{a,1}, Zhiyong Wu^{a,1}, Yingang Feng^d, Feibo Xie^a, Chengwu Liu^a, Jianquan Qin^c, Hongbo Chen^{a,*}

^a State Key Laboratory of Fine Chemicals, School of Chemistry, Dalian University of Technology, No. 2, Linggong Road, Dalian 116012, People's Republic of China

^b State Key Laboratory of Natural and Biomimetic Drugs, Peking University, Beijing 100191, People's Republic of China

^c School of Life Science and Technology, Dalian University of Technology, Dalian 116024, People's Republic of China

^d Qingdao Institute of BioEnergy and Bioprocess Technology, Chinese Academy of Sciences, Qingdao 266101, People's Republic of China

ARTICLE INFO

Article history:

Received 9 August 2012

Received in revised form

26 October 2012

Accepted 28 October 2012

Available online 7 November 2012

Keywords:

Mcl-1

Small molecule inhibitor

Fragment-based approach

Anticancer

ABSTRACT

Based on a known nanomolar Bcl-2 homology domain 3 (BH3) mimetic 3-thiomorpholin-8-oxo-8H-acenaphtho[1,2-*b*] pyrrole-9-carbonitrile (**1** (S1), MW: 331), we applied a fragment-based approach to obtain BH3 mimetics with improved affinity and improved solubility in a water–ethanol (9:1) cosolvent. After the deconstruction of **1** (S1), we obtained fragment cyanoacetamide (**4**), which was determined to be a ligand efficiency (LE) hot part. After a rational optimization through fragment evolution beginning with fragment **4**, a smaller Mcl-1 inhibitor (*E,E*)-2-(benzylaminocarbonyl)-3-styrylacrylonitrile (**4g**, MW: 288) with a 6-fold increase in affinity compared to **1** was obtained, as predicted by our optimization curve and identified by Mcl-1 protein nuclear magnetic resonance (NMR).

© 2012 Elsevier Masson SAS. All rights reserved.

1. Introduction

Targeting the interface between proteins has huge therapeutic potential, but discovering small molecule drugs that disrupt protein–protein interactions is an enormous challenge [1,2]. Recently, we have focused on the inhibitors of Mcl-1 protein [3]. Mcl-1 is one of the most important targets for BH3 mimetics because of its unique antitumor properties [4–6]. We have previously reported a BH3 mimetic **1** that binds directly to the Mcl-1 protein (structure shown in Fig. 1) [7,8]. Structure-based structure–activity relationship (SAR) studies have been performed to modify **1**, which aimed to obtain more potent inhibitors.

Abbreviations: Bcl-2, B-cell lymphoma 2; Mcl-1, myeloid cell leukemia sequence 1; Bcl-x_L, B-cell lymphoma x long; Bax, Bcl-2-associated x protein; Bak, Bcl-2 homologous antagonist/killer; BH3, Bcl-2 homology domain 3; SAR, structure–activity relationship; FPA, fluorescence polarization assay; K_i, inhibition constant; K_d, dissociation constant; HPLC, high-performance liquid chromatography; ADT, AutoDock Tools; ITC, isothermal titration calorimetry; NMR, nuclear magnetic resonance; ΔG, binding free energy; HAC, heavy atom count; LE, ligand efficiency; PDB, protein data bank.

* Corresponding authors. Tel./fax: +86 411 84986032.

E-mail address: zc Zhang@dlut.edu.cn (Z. Zhang).

¹ These authors contributed equally to this work.

We were successful in obtaining inhibitors with increased affinity [9]. Unfortunately, the solubility of those molecules was as poor as the parent compound **1**. Potent compounds do not necessarily result in good drugs; parameters such as molecular weight (MW) and other physicochemical properties related to pharmacological properties also determine the probability that a compound will succeed as a drug [10–14]. We believe that an alternative method is needed to obtain more drug-like Mcl-1 inhibitors based on **1**.

Fragment-based drug design has significantly developed over the past 10 years [15–17]. A final complex drug candidate may be obtained through simple starting-fragment selection and validation, followed by fragment evolution [18]. Because the physicochemical properties at the very beginning of drug discovery are controlled (MW < 250 Da, Clog P < ~3), the final molecules can remain compliant with the rule-of-five if optimization is performed properly [10,13]. LE is the most important metric to guide this process [18–21]. Although many studies, including both forward and retrospective analysis, have been done to predict the fragment-based drug discovery path, there is still a long way to go before protein–protein interaction inhibitors (PPIs) can be discovered routinely through this method [18,22–25].

Herein, we applied a fragment-based approach to obtain more drug-like Mcl-1 inhibitors based on **1** and tried to rationalize the

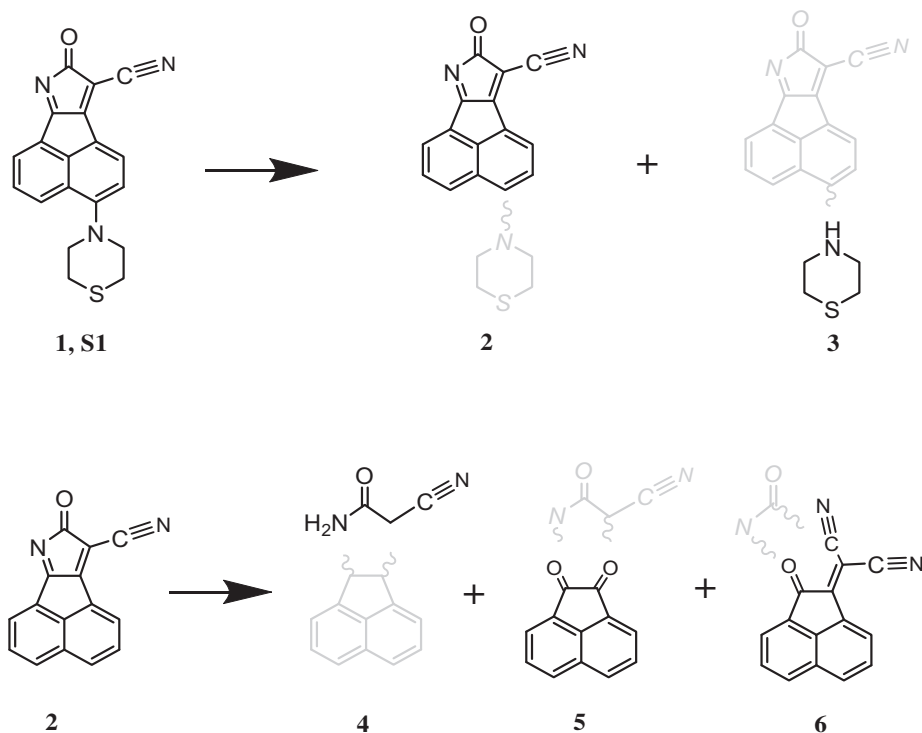


Fig. 1. Deconstruction of **1** into fragments by removing specific groups (highlighted in gray).

fragment-based PPIs design. In addition to obtaining a more potent Mcl-1 inhibitor **4g** with improved solubility compared to **1**, a prediction map for the Mcl-1 inhibitors was constructed through this study, which could benchmark the expectations of upcoming fragment hits with regard to the LE, and enable a better evaluation in the fragment hit selection phase and a subsequent efficient optimization of fragments.

2. Results and discussion

2.1. Deconstruction of **1** into fragments

Our previous investigation has identified **1** as an authentic BH3 mimetic and a nanomolar inhibitor of Mcl-1 ($K_i = 58$ nM by fluorescence polarization assays). To further probe the binding energy contributions of ligands and to construct a prediction map for lead optimization toward Mcl-1 inhibitors, as well as to develop more drug-like Mcl-1 inhibitors, we performed dissection of **1** into smaller fragment molecules, identification of a starting point with the best potential, and fragment optimization.

In the dissection process of **1**, fragments 8-oxo-8H-acenaphtho[1,2-*b*]pyrrole-9-carbonitrile (**2**) and thiomorpholine (**3**), shown in Fig. 1, were first obtained. The binding affinities (K_d) of the compounds were evaluated using isothermal titration calorimetry (ITC) assays. The known Mcl-1 inhibitor Gossypol was used as a positive control. When Gossypol exhibited 2.65 μ M in ITC assay, the K_d value of **1** was 0.96 μ M toward Mcl-1 protein and that of **2** was 1.83 μ M, while no binding to Mcl-1 was determined for **3** ($K_d > 1000$ μ M). The K_d values of compounds to Mcl-1 are outlined in Table 1.

It is well established that a fragment usually obeys a rule of three (MW < 300 Da, Clog *P* < 3, hydrogen bond donors and acceptors each < 3) [25]. For a starting fragment, smaller and more hydrophilic property is better as this may allow for additional manipulations before the final molecular weight becomes too large.

Accordingly, we continued to break down **2** into the fragments cyanoacetamide (**4**), acenaphthequinone (**5**) and 2-[2-oxo-2H-acenaphthylen-1-ylidene]-malononitrile (**6**), shown in Fig. 1. Among them, **4** exhibited the most potent binding ability, where K_d was 13.52 μ M (Table 1). Compounds **5** and **6**, however, were much weaker ($K_d = 324.69$ and 52.25 μ M, respectively).

2.2. Measurement of ligand efficiencies

Affinity is no longer the first consideration in the starting fragment selection [18]. For a starting fragment, a relatively high LE is favorable. Thus, the LE for all of the destructed compounds with detectable K_i value was calculated using following equation [20]:

$$LE = \Delta G / HAC \left(\text{units} = \text{kcal mol}^{-1} \text{ per heavy atom} \right)$$

where binding free energy (ΔG) is derived from equation of $\Delta G = -RT \ln K_d$, and the heavy atom count (HAC) is the number of non-hydrogen atoms in the molecules. As shown in Table 1, we found that the LE for **2** (0.44) was even higher than **1** (0.34), while the LE of **3** was less than 0.01. Clearly, a key interaction was formed by fragment **2**. Fragment **4**, the smallest part of **2**, exhibited the highest LE (1.12). It suggested that **4** contained a high proportion of atoms that made favorable contacts with the Mcl-1 protein. In our previous SAR studies, docking studies, and solution-based binding studies [9], we found the carbonyl group of **1** binds closely to the R263 residue of Mcl-1, and a hydrogen bonding network could be formed between them. It has been established that the R263 group in Mcl-1 is a crucial residue for binding because it can form a salt bridge with D67 in the Bim peptide [26]. Consistently, alanine scanning data showed that only when the G66 and D67 in Bim were mutated, was a significant reduction in binding observed [27]. Here, in order to confirm that such a small fragment **4** indeed bind with Mcl-1 through its interaction with R263, we designed a Mcl-1

Table 1
Fragments from the deconstruction of **1** and their derivatives: name, structure and binding affinity by ITC assays (K_d , μM).

Compound	Structure	K_d (μM)	pK_d	ΔG (kcal/mol)	HAC	LE
Gossypol		2.65	5.58	7.66	38	0.20
1		0.96	6.02	8.27	24	0.34
2		1.83	5.74	7.88	18	0.44
3		>1000	No	No	6	No
4		13.52	4.87	6.69	6	1.12
5		324.69	3.49	4.79	14	0.34
6		52.25	4.28	5.99	18	0.33
4a		2.21	5.66	7.77	13	0.60
4b		1.06	5.97	8.21	15	0.55
4c		8.27	5.08	6.98	7	1.00
4d		6.65	5.18	7.11	8	0.89
4e		4.28	5.37	7.38	9	0.82

Table 1 (continued)

Compound	Structure	K_d (μM)	pK_d	ΔG (kcal/mol)	HAC	LE
4f		1.58	5.80	7.97	13	0.61
4g		0.16	6.80	9.34	22	0.42
6a		4.24	5.37	7.38	26	0.28
6b		4.93	5.31	7.29	27	0.27
6c		3.71	5.43	7.46	28	0.27
6d		1.45	5.84	8.02	30	0.27

R263A mutant to perform ITC to test the affinity of **4**. When **4** exhibited a K_d value of 13.5 μM toward wild type Mcl-1 protein, almost no binding was found with the Mcl-1 mutant. It confirmed that **4** bound Mcl-1 through an interaction with R263. By contrast, fragment **6** exhibited nearly the same K_d value for wild type and mutant Mcl-1 in ITC (Table 2 and Fig. 2). It suggested that **6** had no interaction with R263.

Thus, fragments **2** and **4** showed higher LE than **1** due to the presence of cyanoacetamino group, while **5** and **6** lost most of the

Table 2
Binding affinity of compounds with Mcl-1 and R263A mutant by ITC assays (K_d , μM).

Ligand	Mcl-1	R263A
Gossypol	2.65	
4	13.52	>1000
4f	1.58	90.83
4b	1.06	46.17
4g	0.16	6.72
6	52.25	51.39

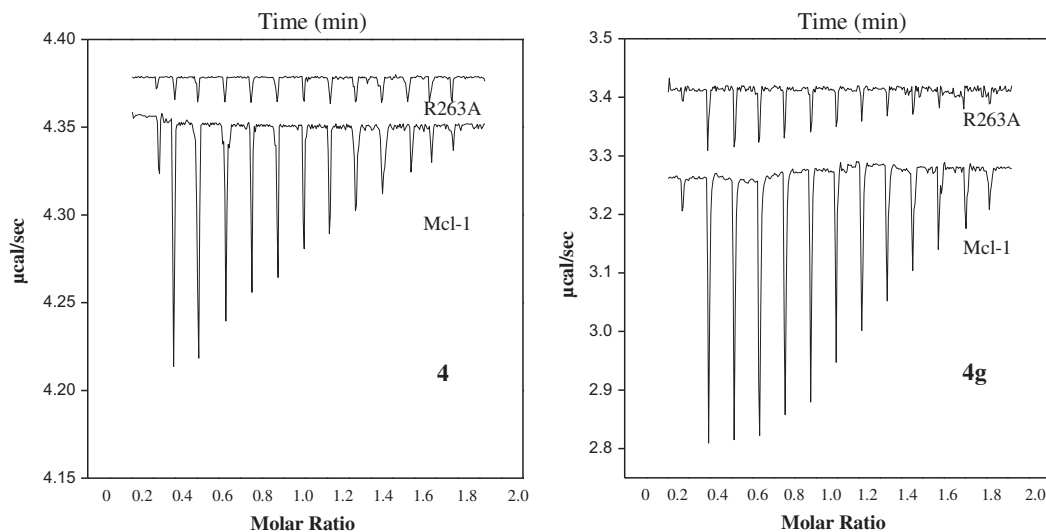


Fig. 2. The binding affinities of **4** and **4g** to wild type Mcl-1 and R263A mutant, respectively determined by ITC. Each peak corresponds to one injection. K_d value was calculated from integration of the raw data (Figure S2).

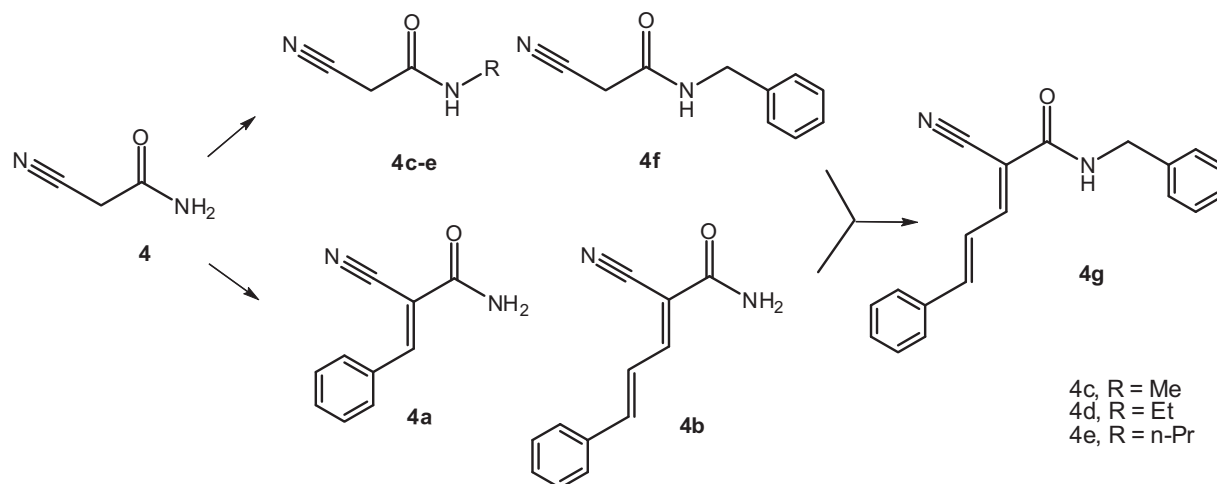


Fig. 3. The path of optimization from fragment **4**.

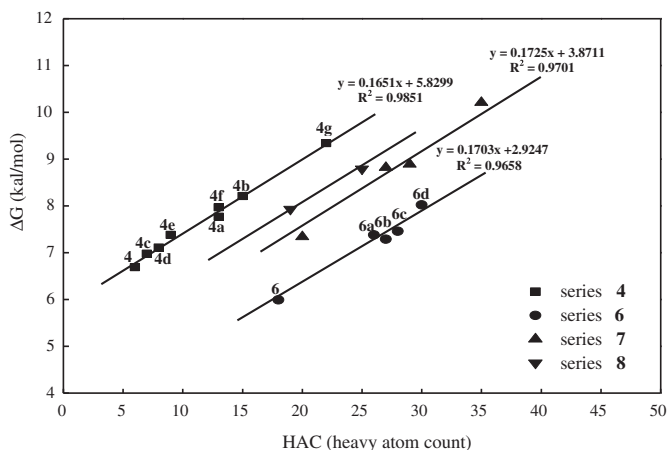


Fig. 4. Free energy of binding (in kcal mol⁻¹) for compounds of series **4**, **6**, **7** and **8** plotted as a function of the number of heavy atoms in the ligands. See Table 1.

affinity because of the lack of this functional group. Fragment **4** has been clearly identified with the highest LE and specific binding site. As such, it was termed an LE hot part that can occupy an LE hotspot in Mcl-1 BH3 domain and it was an ideal starting fragment for further optimization according to de Esch [21]. Although the LE of **6** (0.33) was not as high as for **4** (1.12), the mass (MW = 230) and potency ($pK_d = 4.28$) of **6** still made it an acceptable starting fragment according to the prediction map of Hajduk [18].

2.3. Optimization of fragment **4** and **6** as a starting point

We then optimized from **4** and **6**, separately because we were interested in comparing the two optimization paths that started from fragments with different LE value. We aimed to construct a prediction map for lead optimization toward Mcl-1 inhibitors and enabled a better evaluation of the fragment optimization to obtain a more drug-like candidate.

Firstly, we used fragment **4** as a starting point. According to the binding mode of **4** with Mcl-1, when a hydrogen bond was formed

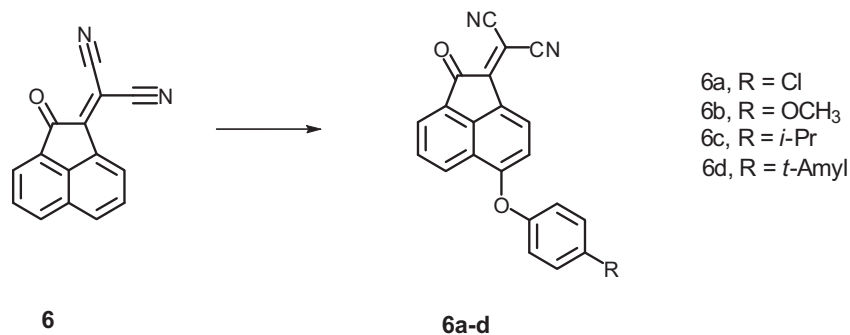


Fig. 5. The path of optimization from fragment 6.

between R263 and carbonyl group, the cyano group was directed to p2 pocket and the amino was adjacent to the p4 (supplementary material Fig. S1). We then attached larger molecular size groups to position 2 and to the amino group of fragment 4 to occupy the p2 and the p4 pocket, respectively. Specifically, we synthesized (*E*)-2-cyano-3-phenyl-2-propenamide (**4a**), (*E,E*)-2-cyano-5-phenyl-2, 4-pentadienamide (**4b**) to occupy p2 pocket, *N*-methyl-2-cyanoacetamide (**4c**), *N*-ethyl-2-cyanoacetamide (**4d**), *N*-*n*-propyl-

2-cyanoacetamide (**4e**), and *N*-benzyl-2-cyanoacetamide (**4f**) to occupy p4 pocket, respectively (Fig. 3).

The K_d values of these compounds against Mcl-1 were evaluated by ITC assays (Table 1). A progressive increase in molecular size of the products resulted in a corresponding improvement in K_d value via ITC. The K_d value of **4a** was 2.21 μ M, while **4b** showed a two-fold higher affinity (1.06 μ M). As to the compounds **4c–f** which were aimed to occupy p4 pocket, a 5-fold decrease in K_d was found in

Table 3
Compounds in series 7 and 8: name, structure and binding affinity by FPAs (K_i , μ M).

Compounds	Structure	K_i (μ M)	pK_i	ΔG (kcal mol ⁻¹)	HAC	LE
7		0.037	7.43	10.21	35	0.29
7a		4.60	5.34	7.34	20	0.37
7b		0.38	6.42	8.82	27	0.33
7c		0.34	6.47	8.89	29	0.31
8		0.018	7.74	10.63	44	0.24
8a		1.69	5.77	7.93	19	0.42
8b		0.40	6.40	8.79	25	0.35

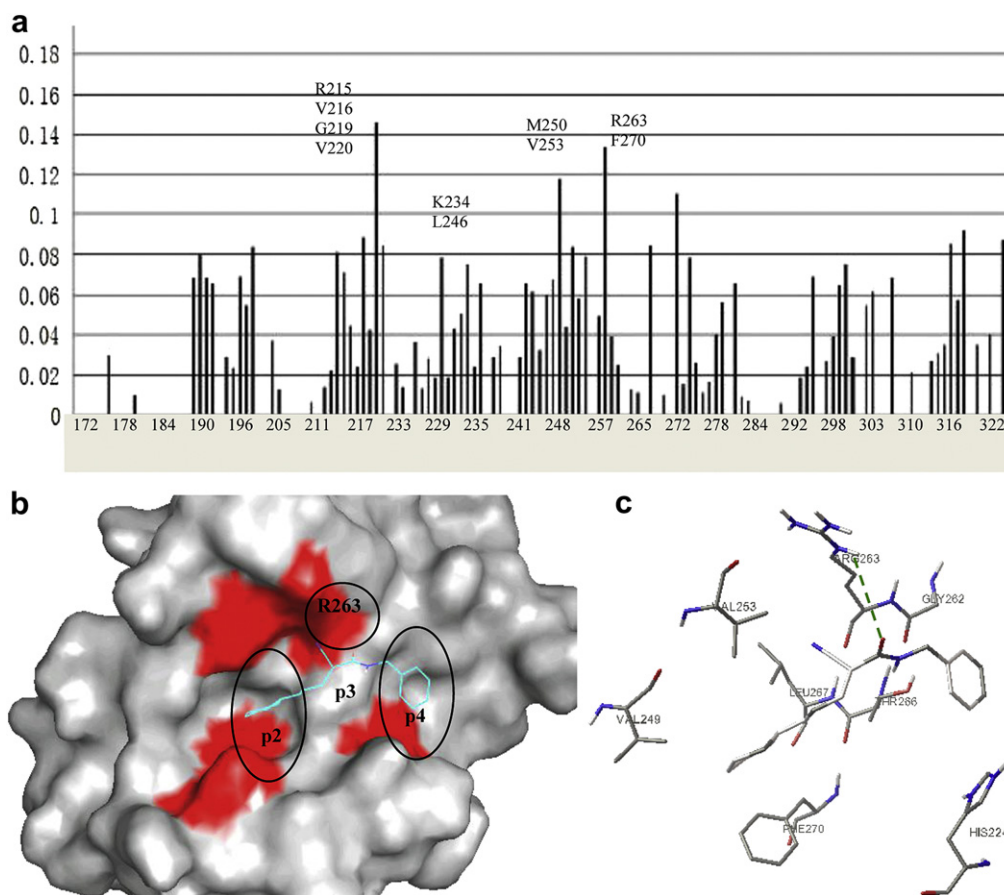


Fig. 6. Binding site of **4g** with Mcl-1 determined by NMR and molecular docking. (a) Amide proton and nitrogen CCSP of Mcl-1 derived from the ^1H – ^{15}N HSQC spectra after titration with **4g** to Mcl-1. (b) Mcl-1 surface is colored according to chemical shift perturbation (red, residues with CCSP ≥ 0.08 ppm upon complexation). (c) The docked structure of **4g** interacted with surrounding residuals. Hydrogen bonds are depicted as green dashed lines. (For interpretation of the references to colour in this figure legend, the reader is referred to the web version of this article.)

going from **4c** (8.27 μM) to **4f** (1.58 μM). In order to monitor the binding mode of these compounds during molecular growing, we evaluated the K_d values of **4b** and **4f** against wild-type Mcl-1 and R263A mutant, respectively by ITC. When **4b** and **4f** showed affinity toward wild-type Mcl-1 (1.16 and 1.58 μM , respectively), a 40- and 60-fold decrease of affinity was found for them toward R263A mutant (Table 2), indicating compounds of series **4** maintained the binding to R263 as fragment **4** did.

To monitor the efficiency during fragment growing, we plotted the ΔG against the HAC. As shown in Fig. 4, a linear ($R^2 = 0.98$) relationship between potency and HAC was found for compounds **4a**–**f**, which had a slope of approximately 0.17 kcal mol $^{-1}$ per additional heavy atom. This slope was defined as V_x . It suggested that the binding mode was conserved upon elaboration of the starting fragment; therefore, the modification sites were appropriate. This encouraged us to further increase the molecular weight to achieve better potency. We merged **4b** and **4f** to yield **4g**. An approximately 10-fold decrease in K_d value for **4g** (0.16 μM) was detected compared to **4b** and **4f**, and more than 100-fold decrease compared to **4** (Table 1). Consequently, we were interested in knowing whether **4b** and **4f** merged efficiently. Simply adding the free energies of binding of **4b** ($\Delta G = 8.21$ kcal mol $^{-1}$) and **4f** ($\Delta G = 7.97$ kcal mol $^{-1}$) provided 16.18 kcal mol $^{-1}$ [28,29]. The overlap of the structural group of **4b** and **4f** was compound **4**, with a ΔG of 6.69 kcal mol $^{-1}$ that should be deducted from the whole energy. Thus, we obtained 9.49 kcal mol $^{-1}$, which was very close to the actual ΔG of **4g** (9.34 kcal mol $^{-1}$). This implied that additivity

was indeed achieved and the binding mode was probably conserved. Notably, $\Delta G/\text{HAC}$ of **4g** was predicted by the linear trend of fragment elaboration of series **4** since it was located exactly on the trend line (Fig. 4). Further, it provided evidence that the fragment-binding mode was conserved upon elaboration.

To further identify the inhibition of **4g** against the Mcl-1 protein, ITC was performed with **4g** and **1** in parallel. **4g** exhibited $K_d = 0.16$ μM , which was 6-fold improved than that of **1** ($K_d = 0.96$ μM , Table 1 and Fig. S2). We also performed ITC with Mcl-1 and Mcl-1 R263A mutant, respectively. Results showed that the R263A mutant weakened the binding of **4g** to Mcl-1 by 40-fold (Fig. 2 and Table 2). It further supported that **4g** maintained the binding model of the initial fragment **4**.

Secondly, fragment **6** was used as an alternative starting point. We used our previous strategies to attach 4-chlorophenoxy, 4-methoxyphenoxy, 4-isopropylphenoxy, and 4-tert-amylphenoxy groups to the 6 position of compound **5** to yield 2-[2-oxo-2H-6-(4-chlorophenoxy)acenaphthylen-1-ylidene]-malononitrile (**6a**), 2-[2-oxo-2H-6-(4-methoxyphenoxy)acenaphthylen-1-ylidene]-malononitrile (**6b**), 2-[2-oxo-2H-6-(4-isopropylphenoxy)acenaphthylen-1-ylidene]-malononitrile (**6c**), and 2-[2-oxo-2H-6-(4-tert-amylphenoxy)acenaphthylen-1-ylidene]-malononitrile (**6d**), respectively (Fig. 5). In our previous SAR studies, we successfully explored the p2 pocket of Mcl-1 by using these groups [9]. Similar to the ITC results of series **4**, a progressive increase in HAC (**6d** > **6c** > **6b** > **6a**) resulted in a corresponding increase in Mcl-1 affinity (Table 1). The K_d value of the final compound **6d** (1.45 μM)

showed a 36-fold enhanced affinity compared to compound **6** (52.25 μM). Moreover, series **6** also exhibited a linear ($R^2 = 0.98$) relationship between potency and HAC (Fig. 4). Notably, this trend line was nearly parallel to that of series **4**. Furthermore, we compared these optimization processes to series **7** (TM-179, structures shown in the Supplementary materials Section, Fig. S4). The K_i values are shown on Table 3 [30], analogs of Gossypol, which are reported excellent inhibitors for Mcl-1, and series **8** (BI33, Fig. S5 and Table 3) [31]. Although the compounds in series **7** and **8** were not based on fragment screening, the modification procedure was also a molecular growing process. These two series of compounds produced, respectively, an approximately constant increase of 0.17 kcal mol⁻¹ per additional heavy atom, which was in good qualitative agreement with the slope of series **4** and **6** (Fig. 4). Additionally, this slope was similar to other reported protein–protein inhibitors (0.24 kcal mol⁻¹ per heavy atom) [2]. The parallel trend lines along the fragment growing in these series of compounds suggested that the average contribution per atom added was equal regardless of whether or not the start fragment was an LE hot part. Consistently, retrospective analyses of 18 known inhibitors showed that all the series of molecules exhibited a nearly paralleled linear relationship between binding affinity and molecular weight. Their slope is also a constant.

Moreover, the linear relationship between the ΔG and the HAC in the three optimization processes suggested that the initial fragments most probably maintained their binding mode, and thus contributed additively to the final ΔG . Although it was not always the case in fragment-based drug discovery, we did find it in these Mcl-1 inhibitors. Because the binding mode could be conservative, the structure and size of the starting point had a decisive effect on the final elaborated compounds.

Notably, although the affinity of **6d** was significantly improved through the molecular growing, the poor solubility (Clog $P = 6.1$) still filtered it out by the rule-of-five. However, **4g** was a molecule that conserved the rule-of-five and had a MW of 288 and a Clog P of 3.5. Compared with its parent compound **1**, **4g** exhibited a more than 10% smaller size but a 6-fold enhancement in affinity. A wider “molecular weight window” was available for it to allow for the later optimization to meet other drug-like properties, such as pharmacokinetics (PK).

2.4. SAR of **4g** by NMR

In order to visualize the binding model of **4g** toward Mcl-1 protein, we produced uniformly ¹⁵N-labeled Mcl-1 protein and measured two-dimensional [¹⁵N, ¹H] NMR spectra in the absence and presence of **4g**, respectively. Many residuals within 171–328 amino acids were found occurring chemical shift perturbation (CCSP). Fig. S3a showed an overlay of the spectra before (blue) and after (red) the addition of **4g**, together with close-up views of selected residues that underwent large chemical shift changes in the presence of **4g** (Fig. S3b). A plot of the chemical shift perturbations against the overall Mcl-1 protein residues was depicted. As shown in Fig. 6a, a cluster of residues in p2 including R263, V253, L246, M250, F270 and K234 experienced average CCSP changes of at least 0.07 ppm. Another cluster of residues in p4 including V220, R215, V216 and G219 experienced CCSP changes of at least 0.06 ppm. Mapping of residuals with highest CCSP, including V253, R263, F270, L246, V220, V216 and R215 into the three-dimensional structure of Mcl-1 showed that those residuals were frequently located within and surrounding the p2, p3 and p4 pocket (Fig. 6b). The residual R263 was also among the most affected residuals upon **4g** binding. When compared with the docked geometries of **4g**, which gained the highest chemscore value (Fig. 6c), the mapping data revealed a fairly good agreement. During docking, the carbonyl

group of **4g** located near R263, hence forming the only hydrogen bound.

2.5. The selective binding of **4g** to Mcl-1 but not Bcl-2

After we succeeded to grow a nanomolar Mcl-1 inhibitor from an LE hot part, we were interested to test its Bcl-2 inhibition. According to our previous studies, the parent compound **1** exhibited a K_i value of 310 nM toward Bcl-2 protein in FPA. However, **4g** lost all the affinity toward Bcl-2 in the FPA (Fig. S6). Actually, fragment **4** did not showed measurable K_i value in FPA, which meant Bcl-2 was lost from the very beginning. Recent studies have reported a Mcl-1-specific ligand Bim F69A/L62A mutant, which lost Bcl-2/Bcl-x_L binding but still retained Mcl-1 binding [27]. This illustrated there is the difference, albeit small, between the BH3 groove of Mcl-1 and Bcl-2/Bcl-x_L.

2.6. **4g** selectively induces apoptosis in Mcl-1-dependent cancer cells

To confirm the specificity of **4g** for the Mcl-1 protein in cellular models, we analyzed its activity in four cell lines. NCI-H23 cells are dependent on Mcl-1 for survival. In contrast, HL-60 cells are Bcl-2-dependent cells and H22 and MCF-7 cells are dependent on both Mcl-1 and Bcl-2. These cell lines were treated with different concentrations of **4g**, and then apoptosis was determined by Annexin V flow cytometry. Fig. 7a showed western blot analysis of the expression levels of Bcl-2 and Mcl-1 in these cell lines. After 48 h treatment, **4g** induced apoptosis in NCI-H23 cells ($\text{IC}_{50} = 0.38 \mu\text{M}$) was 100-fold greater than that in HL-60 cells ($\text{IC}_{50} = 47.2 \mu\text{M}$, Fig. 7b), consistent with its binding selectivity for Mcl-1 over Bcl-2. The response of **4g** in H22 ($\text{IC}_{50} = 3.2 \mu\text{M}$) cells and MCF-7 cells ($\text{IC}_{50} = 5.4 \mu\text{M}$) was not as sensitive as in NCI-H23 cells.

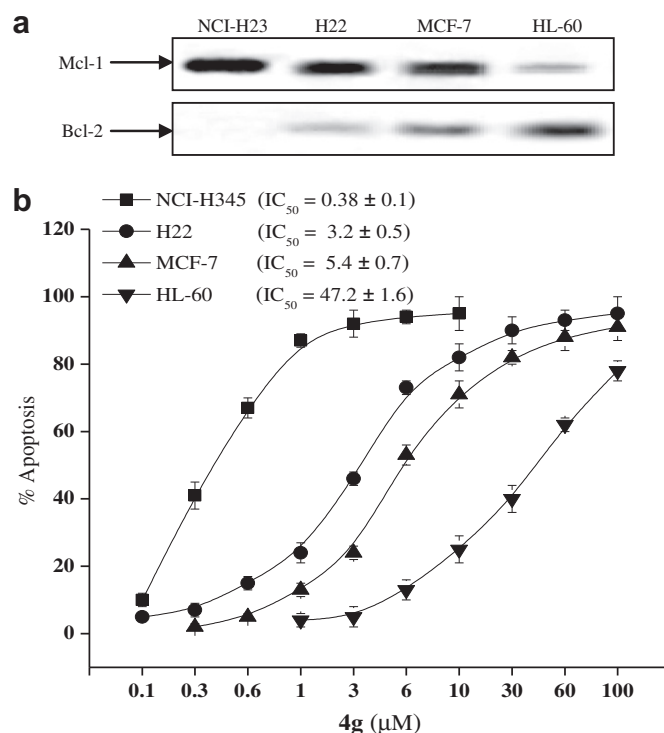


Fig. 7. **4g** induces apoptosis in Mcl-1-dependent cells. (a) The levels of Mcl-1 and Bcl-2 protein in NCI-H23, H22, MCF-7 and HL-60 cells were examined by western blot. (b) Cells were treated with graded concentration of **4g** for 48 h, and the percentage of apoptotic cells was determined by Annexin V flow cytometry.

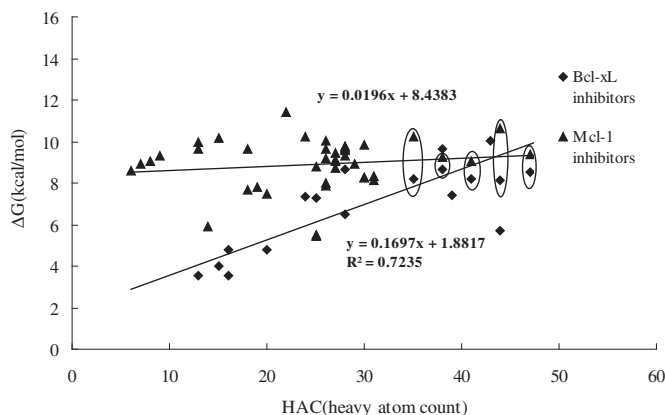


Fig. 8. Free energy of binding (kcal mol^{-1}) for all the reported Bcl- x_L and Mcl-1 inhibitors plotted as a function of the number of heavy atoms in the compounds.

2.7. Comparing the contribution per atom of Mcl-1 inhibitors and Bcl- x_L inhibitors

The very high LE of fragment **4** toward Mcl-1 and the losing Bcl-2 of **4g** raised a possibility that the character of the hotspot of Mcl-1 might be divergent than that of Bcl-2/Bcl- x_L , which may reflect on the LE of their specific ligands. We then surveyed all the reported Bcl- x_L inhibitors and Mcl-1 inhibitors since Bcl- x_L inhibitors are more reported than Bcl-2 inhibitors. All these compounds were listed in Table S1 and S2. Their ΔG against HAC was plotted as shown in Fig. 8. From Fig. 8, we got two lines with different slopes. Additionally, in the case of the Bcl- x_L /Mcl-1 dual inhibitors (circled in Fig. 8), we found that they showed a higher affinity to Mcl-1 than to Bcl- x_L . It suggested that the BH3 groove of Mcl-1 might be more druggable than those of Bcl- x_L .

2.8. Improved solubility of **4g**

According to our previous studies, **1** can only be dissolved in 100% DMSO. Herein, we readily dissolved **4g** in water–ethanol (9:1) cosolvent, which is suitable for oral administration [32,33]. HPLC studies determined that the solubility of **4g** in 100% ethanol was 4 mg/mL at 35 °C and 200 $\mu\text{g/mL}$ in the cosolvent. Conversely, compound **1** can not dissolve in either 100% ethanol or in a water–ethanol (9:1) cosolvent. The increased solubility indicated the improved drug-like properties of **4g** compared to **1**.

3. Conclusion

Following a fragment-based molecule design, we not only rationalized the design of a Mcl-1 protein inhibitor, but also obtained a more drug-like candidate, **4g**. It exhibited $K_d = 0.16 \mu\text{M}$ toward Mcl-1, obtained by ITC assays, which represented a 6-fold enhancement compared to its parent compound **1**. The smaller size and improved solubility in a water–ethanol (9:1) cosolvent made it more favorable for future drug development.

4. Experimental

4.1. Compound synthesis

The synthesis of **4g** is shown in Supplementary material Scheme S2. Yield: 339 mg, 59%. $^1\text{H NMR}$ (400 MHz, CDCl_3): δ 8.94 (br, t, $J = 6.0$ Hz, 1H), 8.02 (d, $J = 11.6$, 1H), 7.71 (d, $J = 4.2$ Hz, 1H), 7.69 (s, 1H), 7.16–7.51 (m, 10H), 4.40 (d, $J = 6.0$ Hz, 2H). TOF MS (EI+):

$\text{C}_{19}\text{H}_{16}\text{N}_2\text{O}$, calcd for 288.1263, found 288.1269. $^{13}\text{C NMR}$ (400 MHz, CDCl_3): δ 160.25, 153.60, 147.97, 137.18, 133.57, 132.45, 130.91, 129.10, 128.90, 128.35, 127.91, 123.06, 115.83, 105.51, 44.42. TOF MS (EI+): $\text{C}_{19}\text{H}_{16}\text{N}_2\text{O}$, calcd for 288.1263, found 288.1269. HPLC system: purity = 99.75%, $t_R = 17.20$ min.

4.2. Isothermal titration calorimetry

Isothermal titration calorimetry (ITC) was performed using iTC200 (Microcal). Experiments were performed in 20 mM Tris pH 8.0, 150 mM NaCl, 1% DMSO at 25 °C. Titrations consisted of $12 \times 3 \mu\text{L}$ injections of compound at 300 μM into Mcl-1 (30 μM). All sample data obtained after control data corrections were analyzed to fit to a one-site model. For control ITC experiments, the sample cells were filled with assay buffer and the compound solution was added. This process was identical to that for protein samples.

Acknowledgments

The authors would like to thank Prof. Zhongjun Li (State Key Laboratory of Natural and Biomimetic Drugs, Peking University, Beijing, People's Republic of China) for the discussion. The work was supported by the Fundamental Research Funds for the Central Universities (DUT11SM08) and partly supported by the National Natural Science Foundation of China (81141099, 81272876).

Appendix A. Supplementary material

Supplementary material associated with this article can be found, in the online version, at <http://dx.doi.org/10.1016/j.ejmech.2012.10.050>.

References

- [1] M.R. Arkin, J.A. Wells, Small-molecule inhibitors of protein–protein interactions progressing towards the dream, *Nat. Rev. Drug Discov.* 3 (2004) 301–308.
- [2] J.A. Wells, C.L. McClendon, Reaching for high-hanging fruit in drug discovery at protein–protein interfaces, *Nature* 450 (2007) 1001–1009.
- [3] S. Cory, D.C. Huang, J.M. Adams, The Bcl-2 family: roles in cell survival and oncogenesis, *Oncogene* 22 (2003) 8590–8607.
- [4] M.F.V. Delft, A.H. Wei, K.D. Mason, C.J. Vandenberg, L. Chen, P.E. Czabotar, S.N. Willis, C.L. Scott, C.L. Day, S. Cory, J.M. Adams, A.W. Roberts, D.C.S. Huang, The BH3 mimetic ABT-737 targets selective Bcl-2 proteins and efficiently induces apoptosis via Bak/Bax if Mcl-1 is neutralized, *Cancer Cell* 10 (2006) 389–399.
- [5] M.R. Warr, G.C. Shore, Unique biology of Mcl-1: therapeutic opportunities in cancer, *Curr. Mol. Med.* 8 (2008) 138–147.
- [6] A.S. Azmi, R.M. Mohammad, Non-peptidic small molecule inhibitors against Bcl-2 for cancer therapy, *J. Cell. Physiol.* 218 (2009) 13–21.
- [7] Z. Zhang, L. Jin, X. Qian, M. Wei, Y. Wang, J. Wang, Y. Yang, Q. Xu, Y. Xu, F. Liu, Novel Bcl-2 inhibitors: discovery and mechanism study of small organic apoptosis-inducing agents, *ChemBioChem* 8 (2007) 113–121.
- [8] Z. Zhang, T. Song, T. Zhang, G. Wu, J. Gao, L. An, G. Du, A novel BH3 mimetic S1 potently induces Bax/Bak-dependent apoptosis by targeting both Bcl-2 and Mcl-1, *Int. J. Cancer* 128 (2010) 1724–1735.
- [9] Z. Zhang, G. Wu, F. Xie, T. Song, X. Chang, 3-Thiomorpholin-8-oxo-8H-ace-naphtho[1,2-b]pyrrole-9-carbonitrile (S1) based molecules as potent, dual inhibitors of B-cell lymphoma 2 (Bcl-2) and myeloid cell leukemia sequence 1 (Mcl-1): structure-based design and structure-activity relationship studies, *J. Med. Chem.* 54 (2011) 1101–1105.
- [10] C.A. Lipinski, Drug-like properties and the causes of poor solubility and poor permeability, *J. Pharmacol. Toxicol. Methods* 44 (2000) 235–249.
- [11] D.F. Veber, S.R. Johnson, H.Y. Cheng, B.R. Smith, K.W. Ward, K.D. Kopple, Molecular properties that influence the oral bioavailability of drug candidates, *J. Med. Chem.* 45 (2002) 2615–2623.
- [12] M.C. Wenlock, R.P. Austin, P. Barton, A.M. Davis, P.D.A. Leeson, Comparison of physicochemical property profiles of development and marketed oral drugs, *J. Med. Chem.* 46 (2003) 1250–1256.
- [13] C.A. Lipinski, Lead- and drug-like compounds: the rule-of-five revolution, *Drug Discov. Today Technol.* 1 (2004) 337–341.
- [14] G. Chessari, A.J. Woodhead, From fragment to clinical candidate—a historical perspective, *Nat. Rev. Drug Discov.* 14 (2009) 668–675.

- [15] D.C. Rees, M. Congreve, C.W. Murray, R. Carr, Fragment-based lead discovery, *Nat. Rev. Drug Discov.* 3 (2004) 660–672.
- [16] P.J. Hajduk, J.A. Greer, Decade of fragment-based drug design: strategic advances and lessons learned, *Nat. Rev. Drug Discov.* 6 (2007) 211–219.
- [17] M. Congreve, G. Chessari, D. Tisi, A.J. Woodhead, Recent developments in fragment-based drug discovery, *J. Med. Chem.* 51 (2008) 3661–3680.
- [18] P.J. Hajduk, Fragment-based drug design: how big is too big? *J. Med. Chem.* 49 (2006) 6972–6976.
- [19] I.D. Kuntz, K. Chen, K.A. Sharp, P.A. Kollman, The maximal affinity of ligands, *Proc. Natl. Acad. Sci. U. S. A.* 96 (1999) 9997–10002.
- [20] A.L. Hopkins, C.R. Groom, A. Alex, Ligand efficiency: a useful metric for lead selection, *Drug Discov. Today* 9 (2004) 430–431.
- [21] S. Schultes, C. de Graaf, E.E.J. Haaksma, I.J.P. de Esch, R. Leurs, O. Kramer, Ligand efficiency as a guide in fragment hit selection and optimization, *Drug Discov. Today* 7 (2010) 157–162.
- [22] D. Tanaka, Y. Tsuda, J. Albert, T. Shiyama, T. Nishimura, N. Chiyo, Y. Tominaga, N. Sawada, T. Mimoto, N. Kusunose, A practical use of ligand efficiency indices out of the fragment-based approach: ligand efficiency-guided lead identification of soluble epoxide hydrolase inhibitors, *J. Med. Chem.* 54 (2011) 851–857.
- [23] G.E. Kloe, D. Bailey, R. Leurs, I.J.P. de Esch, Transforming fragments into candidates: small becomes big in medicinal chemistry, *Drug Discov. Today* 14 (2009) 630–646.
- [24] A. Ciulli, G. Williams, A.G. Smith, T.L. Blundell, C. Abell, Probing hot spots at protein ligand binding sites: a fragment-based approach using biophysical methods, *J. Med. Chem.* 49 (2006) 4992–5000.
- [25] M. Congreve, R. Carr, C. Murray, H. Jhoti, A 'Rule of Three' for fragment-based lead discovery? *Drug Discov. Today* 8 (2003) 876–877.
- [26] P.E. Czabotar, E.F. Lee, M.F. van Delft, C.L. Day, B.J. Smith, D.C. Huang, W.D. Fairlie, M.G. Hinds, P.M. Colman, Structural insights into the degradation of Mcl-1 induced by BH3 domains, *Proc. Natl. Acad. Sci. U. S. A.* 104 (2007) 6217–6222.
- [27] E.F. Lee, P.E. Czabotar, M.F. Delft, E.M. Michalak, M.J. Boyle, S.N. Willis, et al., A novel BH3 ligand that selectively targets Mcl-1 reveals that apoptosis can proceed without Mcl-1 degradation, *J. Cell Biol.* 180 (2008) 341–355.
- [28] C.W. Murray, M.L. Verdonk, The consequences of translational and rotational entropy lost by small molecules on binding to proteins, *J. Comput. Aided Mol. Des.* 16 (2002) 741–753.
- [29] G. Saxty, S.J. Woodhead, V. Berdini, T.G. Davies, M.L. Verdonk, P.G. Wyatt, R.G. Boyle, Identification of inhibitors of protein kinase B using fragment-based lead discovery, *J. Med. Chem.* 50 (2007) 2293–2296.
- [30] G. Tang, Z. Nikolovska-Coleska, S. Qiu, C. Yang, J. Guo, S. Wang, Acylpyrrogallols as inhibitors of antiapoptotic Bcl-2 proteins, *J. Med. Chem.* 51 (2008) 717–720.
- [31] G. Tang, K. Ding, Z. Nikolovska-Coleska, C. Yang, S. Qiu, et al., Structure-based design of flavonoid compounds as a new class of small-molecule inhibitors of the anti-apoptotic Bcl-2 proteins, *J. Med. Chem.* 50 (2007) 3163–3166.
- [32] A. Li, S.H. Yalkowsky, Solubility of organic solutes in ethanol/water mixtures, *J. Pharm. Sci.* 83 (1994) 1735–1740.
- [33] A. Jouyban, J.W.E. Acree, In silico prediction of drug solubility in water–ethanol mixtures using Jouyban-Acree model, *J. Pharm. Pharm. Sci.* 9 (2006) 262–269.